ChemComm

Accepted Manuscript

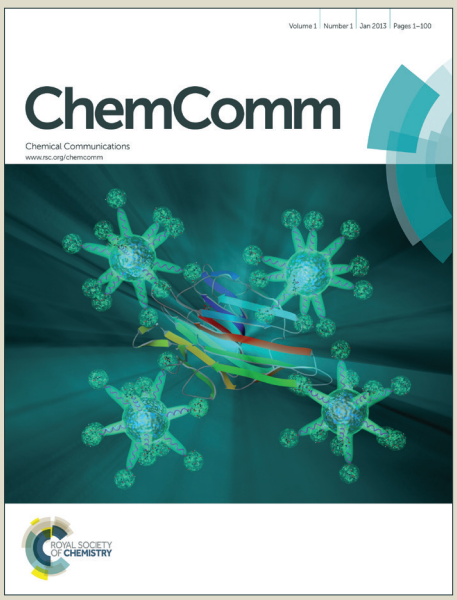

ROYAL SOCIETY OF CHEMISTRY

www.rsc.org/chemcomm

Cite this: DOI: 10.1039/c0xx00000x

www.rsc.org/xxxxxx

ARTICLE TYPE

A Novel Amorphous $CoSn_xO_y$ Decorated Graphene Nanohybrid Photocatalyst for High-Efficient Photocatalytic Hydrogen Evolution

Chao Kong[a,b], Shixiong Min[a,b], Gongxuan Lu[a*]

Received (in XXX, XXX) Xth XXXXXXXXX 200X, Accepted Xth XXXXXXXXX 200X

DOI: 10.1039/b000000x

Novel amorphous cobalt tin composite oxides decorated with graphene nanohybrid ($CoSn_xO_y$/G) sensitized by EY exhibited excellent photocatalytic hydrogen evolution activity (974.6 μmol for 3h) under visible light irradiation. The highest AQE of EY-$CoSn_xO_y$/G of 20.1% was achieved at 430nm.

Photocatalytic hydrogen evolution is one of the most promising routes for the widespread use of the free and sustainable solar energy to develop renewable and clean energy sources[1]. The photocatalytic hydrogen evolution systems usually contain a metal-based cocatalyst, a photosensitizer and a sacrificial electron donor. Among them, cocatalyst is always an attractive and challenging issue and has got more attentions because it offers the low activation potential active sites for H_2 evolution[2-7]. In the reported work so far, noble metals[3], sulfides of transition metals[7], transition metal-based molecular complexes and their derivatives[4-6] are excellent cocatalyst for hydrogen evolution. However, scarcity of noble metals and instability of molecular complexes are still main obstacles in developing stable high-efficient photocatalyst.

Recently, cobalt tin composite oxide has been extensively studied as a promising candidate for Li-ion battery due to its high reversible capacity. It was reported Co_2SnO_4 prepared by hydrothermal method showed high electrochemical performance for Li-ion batteries[8]. Carbon-coated $CoSnO_3$ nanoboxes also exhibited 400 cycles and high-rate capability as an anode material for lithium-ion batteries.[9] However, there have been no reports of cobalt tin composite oxides high catalytic activity for photocatalytic hydrogen evolution.

In the present study, we reported the synthesis of amorphous cobalt tin composite oxides ($CoSn_xO_y$) decorated graphene composite ($CoSn_xO_y$/G) by in-situ chemical deposition and photoreduction. After sensitized by dye, this noble-metal-free photocatalyst exhibited excellent photocatalytic hydrogen production activity under visible light irradiation (λ≥420 nm). In addition, $CoSn_xO_y$/G nanohybrid photocatalyst was insensitive to the reaction pH. The excellent activity might be ascribed to efficient electron transfer via graphene and good activity of $CoSn_xO_y$ for proton reduction.

Photocatalyst preparation details were described in the Supporting Information. Transmission electron microscopy (TEM) images of $CoSn_xO_y$/G nanohybrid (Figure 1 A) displayed that the large amounts of amorphous component adhered on the surface of graphene sheet. In high-resolution TEM (HRTEM) image (Figure 1B), the crystalline nanoparticles had the lattice spacing of 0.33 and 0.26 nm belonged to (110) and (101) planes of tetragonal SnO_2, indicating that the crystalline SnO_2 nanoparticles

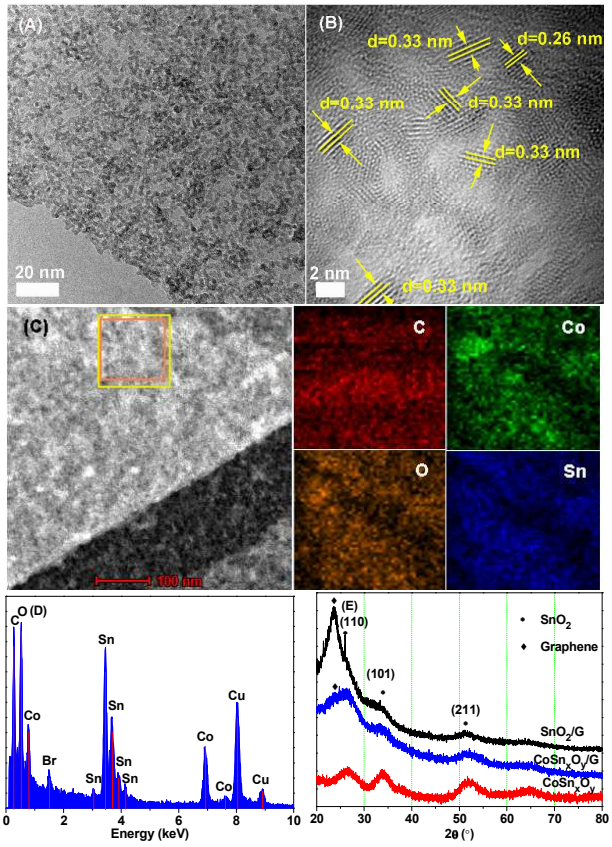

Fig.1 (A) TEM image and (B) HRTEM image for $CoSn_xO_y$/G nanohybrid; (C) HAADF-STEM (high angle annular dark field scanning transmission electron microscopy) image and elemental mapping images of $CoSn_xO_y$/G; (D) EDX spectrum of $CoSn_xO_y$/G, in which the Cu and Br signals originated from the Cu grid support for TEM observation and EY respectively; (E) X-ray diffraction (XRD) patterns of SnO_2/G, $CoSn_xO_y$/G and $CoSn_xO_y$.

were formed in $CoSn_xO_y$/G nanohybrid. Figure 1(C) clearly indicated that the distribution of Co, Sn, C and O element was relatively homogeneous in $CoSn_xO_y$/G. The energy dispersive X-ray (EDX) measurement confirmed the co-existence of Co, Sn, C and O elements in $CoSn_xO_y$/G (Figure 1D). Figure 1(E), which was supported by the X-ray diffraction (XRD) patterns of SnO_2/Graphene (SnO_2/G), $CoSn_xO_y$ and $CoSn_xO_y$/G. These three samples had typical three weak peaks at 26.6°, 33.9° and 51.8°, which belonged to (110), (101) and (211) planes of tetragonal SnO_2 (JCPDS#77-0447) respectively. The peak centered at 2θ =23.6° in XRD patterns of SnO_2/G and $CoSn_xO_y$/G could be assigned to pattern of graphene[10]. No other peaks appeared in Figure 1(E). These results indicated amorphous $CoSn_xO_y$ formed in $CoSn_xO_y$/G nanohybrid and the crystalline SnO_2 nanoparticles existed in $CoSn_xO_y$/G and $CoSn_xO_y$.

XPS spectra of $CoSn_xO_y$/G (Figure 2A) exhibited that the $CoSn_xO_y$/G nanohybrid was mainly consisted of Co, Sn, O and C elements. The binding energies of Co $2p_{3/2}$ (780.9 eV) and Co $2p_{1/2}$ (796.8 eV) in Figure 2(B) indicated Co element was in the +2 oxidation state in $CoSn_xO_y$/G. In Figure 2(C), the peak at 486.5 eV could be assigned to Sn $3d_{5/2}$, while the peak at 494.9 eV could be attributed to Sn $3d_{3/2}$. The presence of both peaks at 486.5 and 494.9 eV indicated Sn element existed in the state of Sn^{4+} in $CoSn_xO_y$/G nanohybrid.

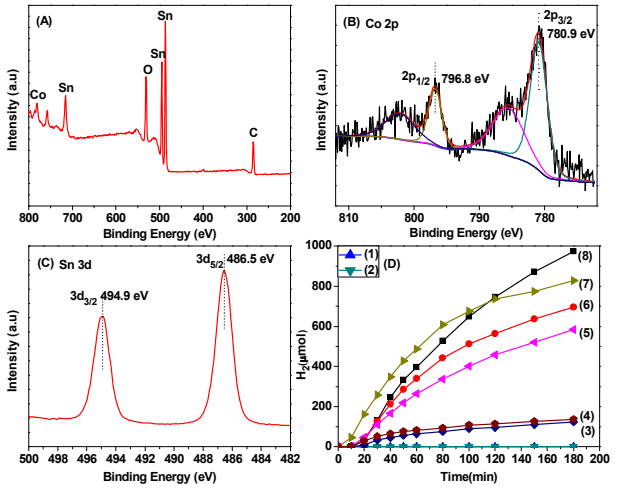

Fig. 2 (A) XPS survey spectra of $CoSn_xO_y$/G. (B) Co 2p scan spectra of $CoSn_xO_y$/G. (C) Sn 3d scan spectra of $CoSn_xO_y$/G. (D) H_2 evolution from EY (1.0×10^{-3} mol/L) photosensitized systems catalyzed by G(1), SnO_2/G(2), Co/SnO_2(3), Co(4), $CoSn_xO_y$(5), Co/G(6), Pt/G(7) and $CoSn_xO_y$/G(8) in 80 mL of 10% (v/v) TEOA aqueous solution (pH=10) under visible light irradiation (λ≥420 nm).

Figure 2(D) showed the time courses of H_2 evolution catalyzed by graphene (G), SnO_2/G, Cobalt/SnO_2 (Co/SnO_2), Cobalt (Co), $CoSn_xO_y$, Cobalt/Graphene (Co/G), Pt/Graphene (Pt/G) and $CoSn_xO_y$/G in 80 mL of 10% (v/v) TEOA aqueous solution under visible light irradiation (λ≥420 nm) at pH 10. As can be seen from Figure 2 (D), only trace amounts of H_2 (0.52 and 0.85 μmol) were produced after 3 h of irradiation in EY-graphene and EY-SnO_2/G system respectively, suggesting that graphene and SnO_2/G were inactive for catalyzing H_2 evolution. The hydrogen productions over EY-Co/SnO_2 and EY-Co were 123.9 μmol and 137.6 μmol in 3h[10], which revealed that the addition of SnO_2 could not enhance hydrogen production activity of Co. The amount of H_2 evolution was 584.4 μmol over the EY-sensitized $CoSn_xO_y$ photocatalyst which was prepared with 450 μL 0.3mol/L $CoSO_4$ and 450 μL 0.3mol/L $SnCl_4$ as precursors. The amount of H_2 evolution was 974.6 μmol over the EY-sensitized $CoSn_xO_y$/G photocatalyst in 3 h, which were 1.67 and 1.4 times higher than that of $CoSn_xO_y$ (584.4 μmol) and Co/G (696.0 μmol) under the same reaction conditions[10]. $CoSn_xO_y$/G also showed higher photocatalytic performance than Pt/G (827.7 μmol) and crystalline $CoSn_xO_y$/G (614.7 μmol) perpared by the hydrothermal method (Figure S1 and S2, ESI†). The high photocatalytic performance of $CoSn_xO_y$/G might be due to the photocatalytic activity of $CoSn_xO_y$ and the electron transfer and separation function of graphene.[7] The optimized $CoSn_xO_y$/G catalyst was prepared via 5 mg of GO, 450μL of 0.3mol/L $CoSO_4$ and 450 μL of 0.3mol/L $SnCl_4$ (Figure S3, ESI†). $CoSn_xO_y$/G always showed good hydrogen evolution performance when mole ratio of Co^{2+} to Sn^{4+} varied in range of 0.5 to 2 (Figure S4, ESI†). The dependence of H_2 evolution activity on pH value indicated $CoSn_xO_y$/G nanohybrid was insensitive to the reaction pH, which exhibited high photocatalytic hydrogen evolution activity in a wide pH range from 8 to 11, and the amount of H_2 evolution was highest at pH 10 (Figure 3A). The small amounts of H_2 (377.3 and 2.05 μmol) were observed when the pH value of the solution was adjusted to 7 and 12. The likely reason was that the concentration of free TEOA to reductively quench EY^{3*} might become low due to the protonation of TEOA in more acidic solutions, while the carboxyl groups of EY might deprotonate in the strong basic solution and the dye could not adsorb on graphene effectively because of the electrostatic repulsion force[11-12].

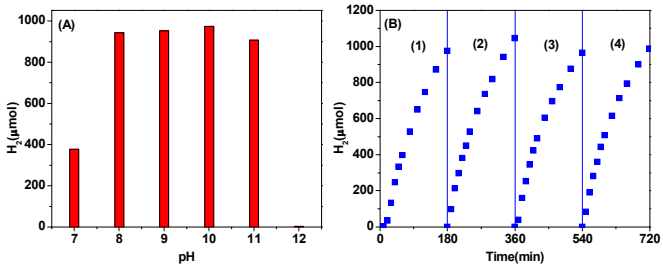

Fig. 3 (A) Effect of pH value on photocatalytic activity of $CoSn_xO_y$/G for hydrogen evolution; (B) Stability test of H_2 evolution over EY sensitized $CoSn_xO_y$/G The reaction was continued for 720 min, with evacuation every 180 min: (1) first run; (2) add EY and evacuation; (3) $CoSn_xO_y$/G was collected by centrifuging from reaction mixture. The recycled $CoSn_xO_y$/G was mixed with TEOA solution and fresh EY, and evacuation; (4) add EY and evacuation.

Hydrogen evolution process usually occurred *via* three steps, including H^+ adsorption, H^+ reduction and H atom desorption in sequence. The adsorption strength of H atom on cocatalyst surface was the key factor for hydrogen evolution reaction, which decided the adsorption and desorption rate of H and formation rate of H_2 molecule over cocatalyst. The H adsorption on Sn^{4+} site was weak while the H adsorption on Co^{2+} was strong, so Co^{2+}

showed high hydrogen generation activity because of its strong adsorption to H[13]. $CoSn_xO_y$ showed the weak adsorption strength of H due to the existence of Sn[14-15], and which should lead to lower photocatalytic activity. However, $CoSn_xO_y$ showed high photocatalytic performance in EY-$CoSn_xO_y$ hydrogen evolution system. There might be related to the hydrogen atom interfacial transfer between Co^{2+} and Sn^{4+} sites in photocatalyst. H^+ might first attach to Co^{2+} site and then gained electron to form H atom, which then transfered from Co^{2+} to Sn^{4+} site, and desorbed to produce H_2 quickly due to the low strength of Sn^{4+}-H. Therefore, $CoSn_xO_y$ showed high photocatalytic activity for H_2 generation.

The stability results of $CoSn_xO_y$/G was shown in Figure 3(B). The dropping of activity was due to decomposition of photosensitizer during photocatalysis with increasing reaction time in the recycle runs (Figure S5, ESI†). The H_2 evolution activity of $CoSn_xO_y$/G could be revived at 98.8% by addition of dye and TEOA. These results showed $CoSn_xO_y$/G nanohybrid was stable during the photocatalytic H_2 evolution processes. Apparent quantum efficiencies (AQEs) from 430 to 550 nm were measured. The highest AQE of EY-CoS_x/G was 20.1% at 430nm (Figure 4A). In Figure 4(B), the higher photocurrent of EY-$CoSn_xO_y$/G indicated the fast electron transfer from $EY^{-}\cdot$ to $CoSn_xO_y$/G, after that, the excited state dye can be reductively quenched by the TEOA to form $EY^{-}\cdot$ species. The graphene induced the fast electron transfer and separation, and as a result, photocatalytic H_2 evolution activity of $CoSn_xO_y$/G was improved[7].

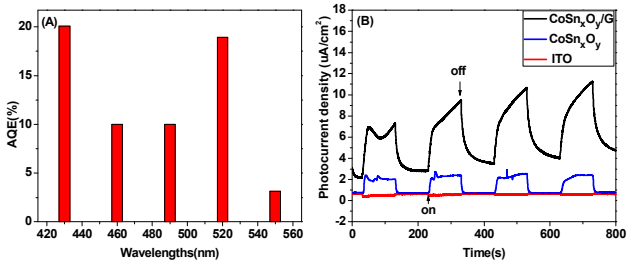

Fig. 4 (A) AQEs of H_2 evolution for EY (1.0×10^{-3} mol/L) photosensitized systems catalyzed by the recycled $CoSn_xO_y$/G nanohybrid. The system was irradiated by a 300-W Xe lamp with a cutoff filter of 420 nm and a bandpass filter. (B) Transient photocurrent-time profiles of EY-$CoSn_xO_y$ and EY- $CoSn_xO_y$/G coated on ITO glass in mixed solution of 10% (v/v) TEOA and 0.1 mol/L Na_2SO_4.

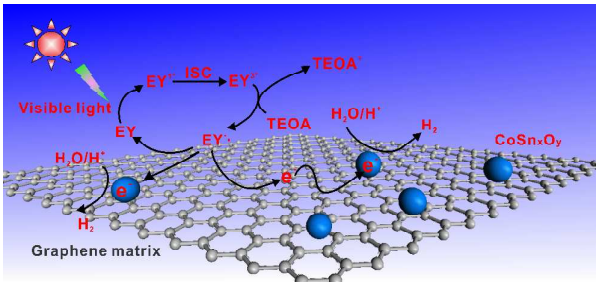

Scheme 1. The proposed photocatalytic mechanism for hydrogen evolution over EY-$CoSn_xO_y$/G photocatalyst under visible light irradiation.

The reaction process of photocatalysis H_2 evolution in EY-$CoSn_xO_y$/G system can be explained as Scheme 1. Under visible light irradiation, the EY on the surface of graphene sheets and $CoSn_xO_y$ absorbs light photon to form singlet excited state EY^{1*}, and then produces the lowest-lying triplet excited state EY^{3*} *via* an efficient intersystem crossing. EY^{3*} can be reductively quenched by TEOA and produce $EY^{-}\cdot$ and oxidative donor ($TEOA^+$) [10-11]. These $EY^{-}\cdot$ species preferentially transfer their electrons to $CoSn_xO_y$ cocatalyst directly or graphene sheets due to its electron transport characteristics. The accumulated electrons on the graphene sheets will transfer to the $CoSn_xO_y$ cocatalyst, finally H^+ obtain electrons from $CoSn_xO_y$ to form hydrogen. The graphene functions as an electron acceptor and transporter to improve the charge separation efficiency, thereby enhancing the catalytic H_2 evolution activity of $CoSn_xO_y$/G nanohybrid.

In summary, $CoSn_xO_y$/G nanohybrid was synthesized by in-situ chemical deposition and photoreduction via Eosin Y photosensitizer, which exhibited excellent photocatalytic performance in a broader pH range from 8 to 11. In addition, $CoSn_xO_y$/G showed higher catalytic activity than Pt/G. $CoSn_xO_y$/G might be a promising alternative for noble metal catalysts in photocatalysis proton reduction.

This work is supported by the 973 and 863 Programs of Department of Sciences and Technology of China (2013CB632404, 2012AA051501, 2009CB220003) and the NSF of China (grant no. 21173242), respectively.

Notes and references

[a]*State Key Laboratory for Oxo Synthesis and Selective Oxidation, Lanzhou Institute of Chemical Physics, Chinese Academy of Science, Lanzhou 730000, China*
[b]*University of Chinese Academy of Science, Beijing 10080, China.*
**Corresponding author: E-mail: gxlu@lzb.ac.cn.*
Tel.: +86-931-4968 178. Fax: +86-931-4968 178.
† Electronic Supplementary Information (ESI) available: [details of any supplementary information available should be included here]. See DOI: 10.1039/b000000x/

1 S. Jasimuddin, T. Yamada, K. Fukuju, J. Otsuki, K. Sakai, *Chem. Commun.*, 2010, **46**, 8466-8468.
2 K. Maeda, K. Teramura, N. Saito, Y. Inoue, K. Domen, *J. Catal.*, 2006, **243**, 303-308.
3 H. Yan, J. Yang, G. Ma, G. Wu, X. Zong, Z. Lei, J. Shi, C. Li,. *J Catal,* 2009, **266**, 165-168.
4 J.P. Bigi, T.E. Hanna, W.H. Harman, A. Changa , C. J. Chang, *Chem. Commun.*, 2010, **46**, 958-960.
5 O. Pantani, S. Naskar, R. Guillot, P. Millet, E. A. Mallart, A. Aukauloo, *Angew. Chem. Int. Ed.*, 2008, **47**, 9948-9950.
6 L.A. Berben, J.C. Peters. *Chem. Commun.*, 2010, **46**, 398-400.
7 S. Min, G. Lu, *J Phys Chem C*, 2012, **116**, 25415-25424.
8 G. Wang, X.P. Gao, P.W. Shen, *J. Power Sources*, 2009, **192**, 719-723.
9 Z.Y. Wang, Z.C.Wang, W.T Liu, W. Xiao, X.W. Lou, *Energy Environ. Sci.*, 2013, **6**, 87-91.
10 C. Kong, S. Min, G. Lu, *Int. J. Hydrog. Energy.*, 2014. DOI:10.1016/j.ijhydene.2014.01.089.
11 S. Min, G. Lu, *J. Phys. Chem. C*, 2011, **115**, 13938-13945.
12 T. Lazarides, T. McCormick, P. W. Du, G. G. Luo, B. Lindley, R. Eisenberg, *J. Am. Chem. Soc.*, 2009, **131**, 9192-9194.
13 G. Jerkiewicz, *Prog. Surf. Sci.*,1998, **57**, 137-186.
14 H. Yamashita, T. Yamamura K. Yoshimoto, *J. Electrochem. Soc.*, 2012, **37**, 17899-17909.

15 B.M. Jovic, U.C. Lacnjevac, N.V. Krstajic, V.D. Jovic, *Electrochimica Acta*, 2013,**114**, 813-818.